Jurnal Polimesin
Department of Mechanical Engineering
State Polytechnic of Lhokseumawe
http://e-jurnal.pnl.ac.id/polimesin

e-ISSN : 2549-1999 No. : 5 Month : October
p-ISSN : 1693-5462 Volume : 23 Year : 2025

Processing dates: received on 2025-06-21, reviewed on 2025-07-27, accepted on 2025-08-28 and online availability on 2025-10-31

Design and development of a radial air bearing concave profile for an educational tool

Herman Budi harja, Risky Ayu Febriani*, Novi Saksono, M. Yazid Diratama, M. Fauzi
Department of Manufacturing Engineering, Politeknik Manufaktur Bandung, Bandung 40135, Indonesia
*Corresponding Author: riskyayu@me.polman-bandung.ac.id

Abstract

The increasing demand for high-speed, precision machinery has highlighted the limitations of conventional friction and anti-friction bearings, driving the need for more advanced bearing technologies, such as air bearings. However, achieving competency and skills related to air bearing components is difficult to access, particularly radial air bearing rigs. This paper presents the design of a radial air bearing rig as a learning tool to support educational objectives in understanding the working principles, use, and maintenance requirements of air bearing systems. The design stages use the VDI 2222 methodology and utilize SolidWorks for modeling. Air quality specifications refer to the ISO 9001:2015 – New Way Air Bearings standards, which consist of a fly height of 5µm, with operational parameters of 4–6 Bar input pressure and 2–13 LPM flow rate. The rig uses a single-phase motor for shaft rotation and a porous pad for air distribution. The test results show that the rig achieves a fly height of 0.5 µm at 4 Bar pressure and 5 LPM flow rate, although its rotation exhibits resistance. These outcomes confirm the rig's potential as an educational tool and highlight the need for mechanical improvements to enhance its performance.

Keywords:
Radial air bearing, design, VDI 2222, air pressure, flow rate

1 Introduction

Air bearings play a vital role in precision engineering by enabling frictionless motion by utilizing a thin film of pressurized air, offering advantages such as low maintenance, high accuracy, noiselessness, increased stiffness, excellent thermal stability, and extended service life [1], [2]. Nowadays, their application spans across industries, including medical research, high-precision manufacturing, optical grinding, and testing equipment, where conventional bearings often fall short in meeting the demands for speed and precision. A study was done to investigate performance issues encountered in a Coordinate Measuring Machine (CMM), which were determined to originate from deficiencies in the design of its air-bearing system. CMMs encounter dynamic errors due to the limited stiffness of air bearings and Abbe's offsets, which affect their measuring speed. Finite Element Analysis (FEA) was used to optimize the design, significantly reducing these errors [3]. In addition, porous journal air bearings have many potential applications for the design and testing of ultra-precision machine tools, including motion error prediction, structural optimization, and component grinding method selection, which align closely with recent research advancements in spindle design [4], [5]. Such spindles feature both static and dynamic stability, with rotation speeds capable of up to 15000 rpm for machining micro-holes between 0.35 and 2 mm in diameter [6]. This issue arises due to the limited availability of teaching resources, making it difficult for practitioners to implement practical training programs. Such programs can bridge the gap between theoretical knowledge and real-world application, particularly in ensuring that polytechnic graduates are well-prepared for the demands of the working world [7].

This study aims to address the gap by designing and validating a radial air-bearing rig as an educational tool. The rig is intended to support an educational tool by demonstrating the working principles, usage, and maintenance of air-bearing supports. The rig was developed using the Verein Deutscher Ingenieur (VDI) method 2222 design methodology [8] and modeled in SolidWorks, with performance parameters aligned to ISO 9001:2015 – New Way Air Bearings standards. By integrating key components, such as a porous media pad, an air supply system, and a single-phase motor drive, the rig provides a practical platform for understanding air-bearing behavior. Besides, precision rotary motion is achieved through the use of two specific types of radial air-bearing lines: concave and convex [9]. In this study, the designed radial air-bearing rig had a concave profile, as shown in Fig. 1. The expected contribution is a validated educational tool that not only enhances the competencies and skills in precision engineering, but also significantly influences the communication process in the classroom to support real-world skill development [10], [11].

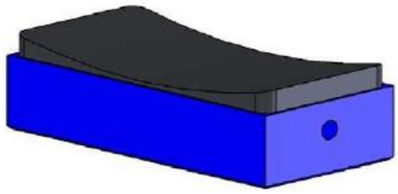

Fig. 1. Concave radial air bearings

2 Research methodology

The design of a concave radial air-bearing rig was carried out through four main stages using the VDI 2222 method, each involving multiple steps. These four stages are planning, conceptualizing, designing, and finalizing, as depicted in the design framework in Fig. 2.

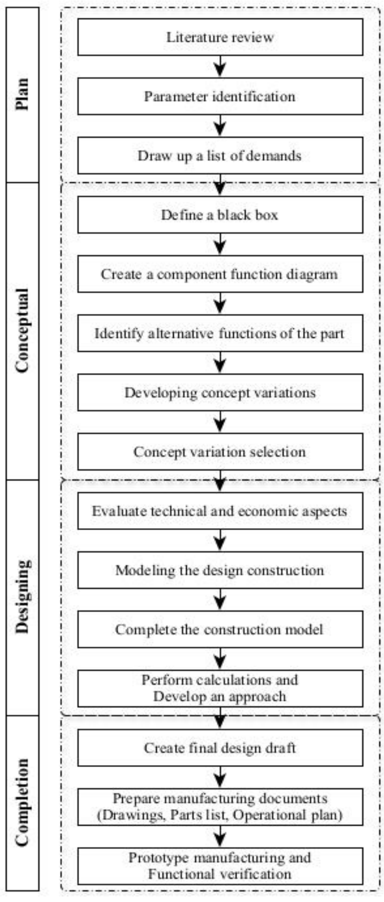

Fig. 2. Design framework of VDI 2222 stages

The initial stage of the design process involved a thorough literature review to understand the fundamental principles of air bearings, with design specifications primarily derived from the ISO New Way Bearing reference. This foundational knowledge was essential to creating an accurate and relevant design. Subsequently, the research parameters for testing the functionality of the radial air bearing were identified to guide the testing process, including fly height, flow rate, pressure, leakage, load capacity, friction, and wear. These parameters were crucial in verifying the rig's performance and suitability for educational use. This resulted in a list of main requirements of high priority, detailed in Table 1.

The second stage is conceptual design, which results in a black box, a function diagram, alternative part functions, alternative combination functions, concept variations, and decision-making outcomes. Material selection is also carried out during this stage, based on the functional requirements of the radial air-bearing rig, such as stiffness, thermal stability, machinability, and compatibility with air-bearing operation.

Table 1. List of main requirements radial air bearing rig

No.	Requirement	Specification
		Construction requirements
1	Manufacturable	Enables to be made
2	Shaft	Cylindrical No corrosion
3	Bracket	Easy setting
4	Air bearing	Able to operate as a shaft support with minimal misalignment
5	Pad	Able to transmit air Not leaking
		System requirements
1	Pressure	Air pressure must be stable within 4-6 bar
2	Load capacity	Air bearings must withstand shaft loads according to specifications without deformation
3	Friction	Minimal friction for increased efficiency

These conceptual designs provide a structured framework for selecting and refining the most feasible design solution. In the third stage, the selected concept design is modeled using SolidWorks, and technical calculations are performed to determine the air pressure and friction for air-bearing systems. This ensured that the design was not only theoretically sound but also practically feasible.

The final stage involves production planning and testing, which includes creating an operation plan, machining processes, and assembling the prototype. The performance of the prototype is evaluated based on predefined parameters. The experimental setup consisted of a regulated air supply system and a load application mechanism that simulated a 2.5 kg shaft load. The rig is considered to meet the standard if it can support a shaft load of 2.5 kg at an input pressure of 4-6 bar, maintain a distance of 95 mm between the base and the shaft's center point, exhibit no leakage, and ensure the distance between the pad and the shaft remains stable within 5 µm. This testing process is crucial as it determines the suitability of the radial air-bearing rig for use as an educational tool that connects theoretical knowledge to practical application.

3 Results and discussion

3.1 Design stages

Based on the developed black box model, the design scheme of the radial air-bearing rig consists of six component functions: pneumatic, bracket, air-bearing operation (including housing pad and pad), transmission, base, motor drive, and shaft rotation. A schematic representation of this radial air-bearing concave design is provided in Fig. 3.

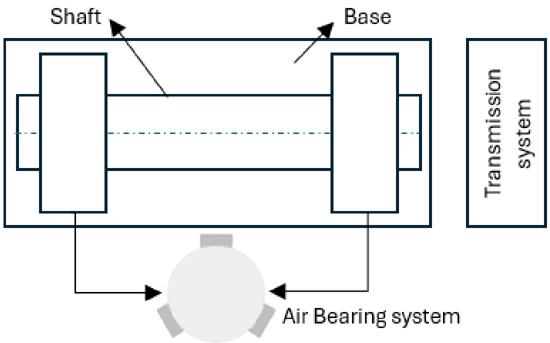

Fig. 3. Concept of rig radial air bearing

3.1.1 Alternative part functions

Alternative component functions in this study refer to various ways or methods to achieve the same function on a particular component in the radial air-bearing construction. The six component functions are then defined to determine which type of system is most effective, resulting in several alternative part functions, as shown in Table 2.

A morphology table is created for each part function by providing an explanation and assessment of the advantages and disadvantages of each alternative part function. Table 3 shows an example of a morphological table for alternative functions of the pad

Table 2. Alternative part functions

Criteria	Alternative			
	1	2	3	4
A. Pneumatic	Filter	Separator		
B. Support	Hexagonal	4-Sided groove	3-Sided groove	
C. Housing pad	Double port inlet	Side single port inlet	Top single port inlet	
D. Pad	Graphite	Aluminum		
E. Transmission	Pulley & belt	Gear	Flange coupling	Sprocket & chain
F. Base	Pin	Slot	JIS C	Threaded hole
G. Motor	3 Phase	Servo	1 Phase	
H. Shaft	Bulk	Hollow		

In an air bearing system, the pad is the main component responsible for distributing air pressure. The use of graphite (EDM 10) was chosen based on test results showing that its porosity allows proper transmission of air pressure. Following material selection, based on the created morphological box, the alternative functions of the parts are combined or grouped into an Alternative Overall Function (AOF), which is divided into four types, as shown in Table 4.

Table 3. Example of a morphological analysis for alternative functions of the pad

Aspect	Material carbon graphite	Material aluminum
	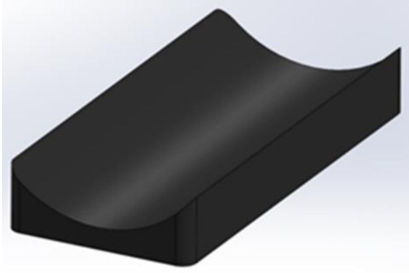	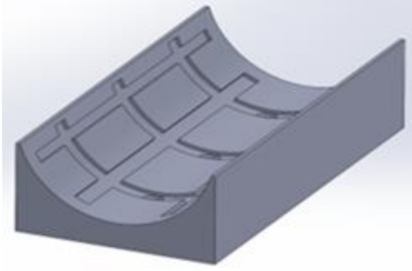
Principle	Air pressure is transmitted through the cavities present in the porous graphite material	Air pressure is transmitted through the grooves present on the surface
Advantages	• Easy machining • More uniform air distribution (across the entire surface)	• Material is easy to obtain • Material costs are more economical
Disadvantages	• Material is difficult to obtain • Higher material costs	• The machining process is difficult • Air distribution is less uniform (across the surface)

Table 4. AOFs

Criteria	Alternative			
	1	2	3	4
A. Pneumatic	A1	A2		
B. Support	B1	B2	B3	
C. House pad	C1	C2	C3	
D. Pad	D1	D2		
E. Transmission	E1	E2	E3	E4
F. Base	F1	F2	F3	F4
G. Motor	G1	G2	G3	
H. Shaft	H1	H2		
Remarks:	AOF_1	AOF_3		
	AOF_2	AOF_4		

3.1.2 Concept variations

The stage of various concepts was developed using morphological methods to identify various combinations of functions that could be integrated into the schematic of this radial air-bearing concave design. Following the development of the morphological chart and the identification of potential concepts, the next step is to present the results in the form of a design. The purpose of these visual representations is to facilitate a comprehensive evaluation of the selected function combinations against the defined technical specifications and needs. The construction results of the combined AOFs are shown in Fig. 4 to Fig. 7.

3.1.3 Decision selection

After obtaining the formulation of AOFs, the next step is the assessment process that will be developed in the design stage. The assessment criteria have a range of values from 0 to 4. It represents the indications of very poor, poor, sufficient, good, and very good. The assessment results of three overall function alternatives based on technical and economic aspects are presented. Table 5 illustrates the assessment of technical and economic aspects of AOF.

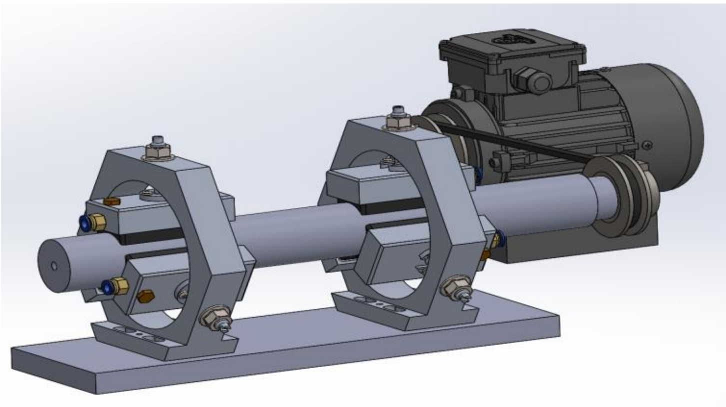

Fig. 4. AOF_1

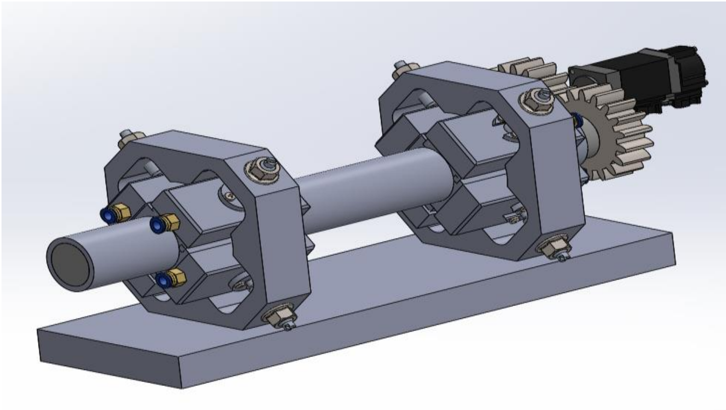

Fig. 5. AOF_2

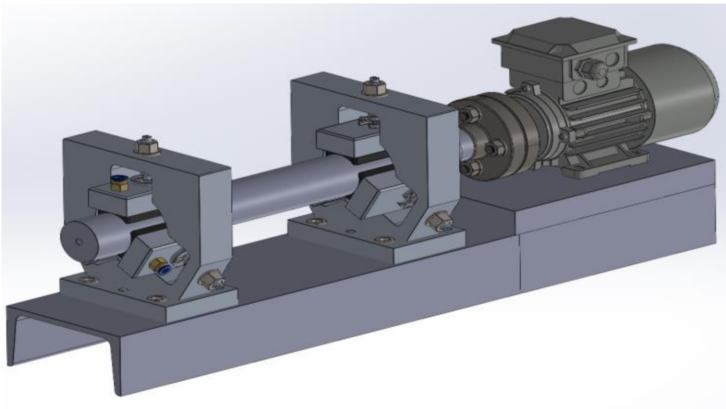

Fig. 6. AOF_3

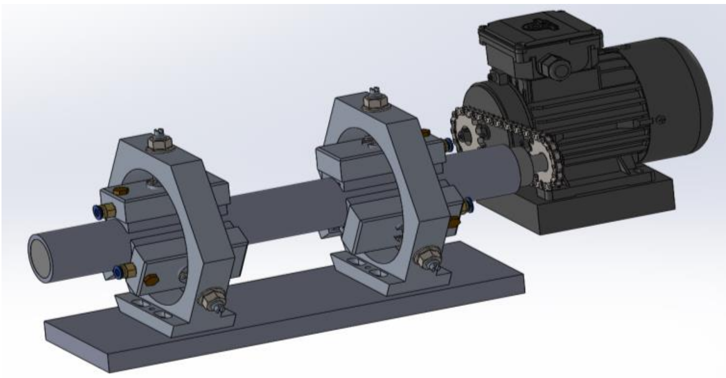

Fig. 7. AOF_4

Based on the assessment of aspects and data on existing concept variations, the ideal combination function from the Table 5 concept variations are AOF_3, with the highest assessment percentage of 81.25%. The next stage is making a draft design for the radial air-bearing concave rig construction, which is divided into nine main parts, as shown in Fig. 8. Furthermore, this construction design was analyzed to obtain further information about the forces acting on the bearing, flow rate, fly height, friction, and rotating shaft.

Table 5. Assessment of technical and economic aspects of AOF

No.	Assessment aspects		Weighting	AOF_1		AOF_2		AOF_3		AOF_4		Ideal score
1	Technical	Function achievement	25	2.3	58.3	2.3	58.3	4	100	2.7	66.7	100
2		Construction	15	2	30	2.3	35	3.3	50	1.7	25	60
3		Operation	10	2.3	23.3	2.3	23.3	3	30	2	20	40
4		Manufacture	20	2.7	53.3	2	40	2.7	53.3	2.3	46.7	80
5		Assembly	5	2	10	2.7	13.3	2.7	13.3	2	10	20
6		Maintenance	5	2.7	13.3	2	10	3.3	16.7	2	10	20
7	Economic	Cost	15	1.7	25	1	15	3	45	2	30	60
8		Standard component	5	3.3	16.7	2.3	11.7	3.3	16.7	3	15	20
Total score			100	230		206.7		325		223.3		400
Percentage			100%	57.5%		51.67%		81.25%		55.82%		100%

Moreover, the detailed design stage was carried out to generate assembly working drawings, detailed working drawings, stages of the work process, and operation plans that will be used as information for the manufacturing process of each component. This stage can also help make the work sequential, making it easier and more systematic.

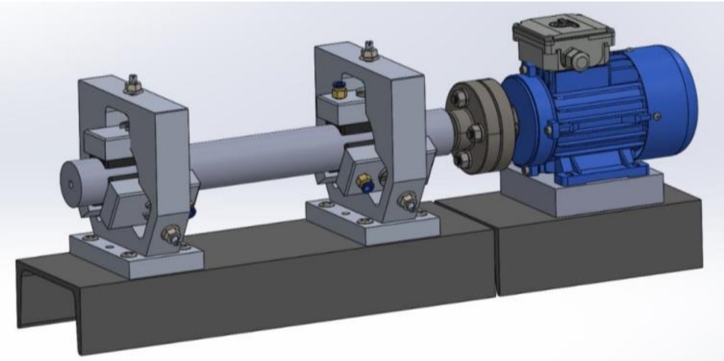

Fig. 8. Construction design of the leak test tool

3.2 Calculation of parameters

3.2.1 Forces acting on the bearing

The calculation of the forces acting on the radial air bearing construction is carried out to determine the load received by the bearing. The shaft is made of duralumin material with a diameter of 25 mm and a length of 450 mm, assuming there are no axial forces, and the only force received is from the mass of the shaft. To calculate the shaft capacity, the volume formula is used Eq. (1) [4], [11].

$$V = \pi \times r^2 \times t \quad (1)$$

$$V = \pi(0.025\ m)^2 \times 0.45\ m = 0.00088357293382\ m^3$$

Then, the calculation of the shaft mass is obtained by multiplying the volume by the density (ρ) of the duralumin, and the shaft mass is converted into force (Eq. (2)).

$$m = \rho \times V \quad (2)$$

$$m = 2780\ ^{kg}/_{m^3} \times 0.00088357293382\ m^3 = 2.456\ kg$$

Converted into Newtons using the standard acceleration due to gravity (9.81 m/s²), can be obtained using Eq. (3).

$$W = m \times g \quad (3)$$

$$W = 2.456\ kg \times 9.81\ m\ /\ s\text{^}2 = 24.09336\ N$$

Fig. 9 and Fig. 10 respectively show the front and side views of the Free Body Diagram (FBD), where the forces generated from the shaft are divided into two for each side of the construction (Eq. (4)).

$$\sum mo = 0 \quad (4)$$

$$(1/2\ F \times 25)$$

$$Fy = \frac{\frac{1}{2} F \times 25\ mm}{50\ mm} = \frac{\frac{1}{2}(24.0933\ N) \times 25\ mm}{50\ mm} = 6.0233\ N$$

$$Fr_1$$

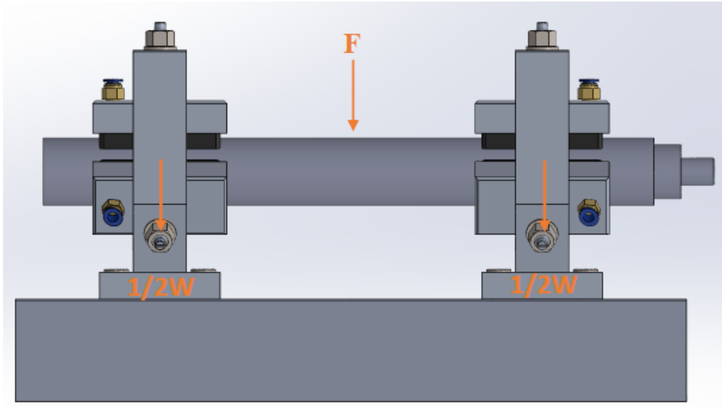

Fig. 9. Front view FBD

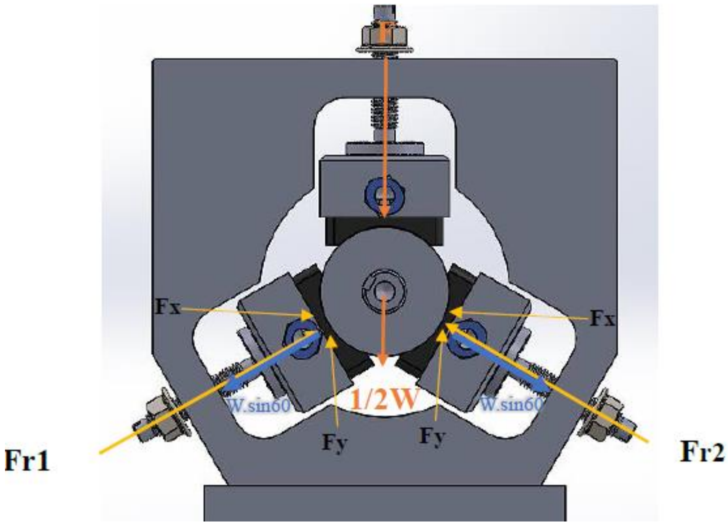

Fig. 10. Side view FBD

Based on the force diagram above, the force received by each pad (bottom) is 6.0233 N. From the force received by the bearing, it can be determined what the surface pressure occurs on each pad. Then, the area is calculated by multiplying the arc length by the width of the object. The surface pressure data can be calculated using Eq. (5).

$$P = \frac{F}{A} \quad (5)$$

$$P = \frac{6.0233\ N}{90\ mm \times 41.222\ mm} = 0.00162\ ^{N}/_{mm^2}$$

The surface pressure of each pad will affect the pressure required during the radial air bearing test. Therefore, it can be assumed that pressure is needed for each bottom pad to lift the load.

Bottom pad $\boldsymbol{p}$ ***output air bearing*** ($\boldsymbol{p_1}$ ***atau*** $\boldsymbol{p_2}$) > $\boldsymbol{p}$ surface pressure $\boldsymbol{P_1}$=$\boldsymbol{P_2}$. The pressure at the output of the air bearing, which has experienced a pressure drop, is crucial in determining its ability to withstand the existing forces. However, the upper pad will not run into surface pressure when the air supply is inactive; pressure will occur when the air supply is active. To balance the upper and lower pressures and achieve equilibrium, the pressure required for the upper pad can be calculated using the following formula: $\mathbf{P_3 = P_1 - P}$ **surface pressure**.

3.2.2 Flowrate

The flow rate in an air bearing is a crucial parameter that affects the performance of the air bearing. Flow rate can affect the thickness of the air film separating the bearing surfaces. Higher flow rates will produce higher air films, thus being able to support greater loads. However, an excessively high flow rate can lead to air wastage and may cause excessive noise. By determining the optimal airflow rate, we can maximize bearing performance without sacrificing air use efficiency. A controlled flow rate can minimize friction and wear, as well as balance stiffness for high-precision applications. After setting the required pressure, the flowmeter is adjusted until the load lifts minimally. Thus, a flow rate (Q) of 1 LPM or 1 dm³/min is obtained. Subsequently, the flow rate (Q) is calculated as an approximation. So, to find out the resulting airflow rate, it can be calculated using Eqs. (6) dan (7) [7], [9], [11].

$$V = \frac{Q}{A} \quad (6)$$

$$V = \frac{1\,dm^3/min}{28.274\,mm^2} = \frac{0.0000167\,m^3/s}{0.0000282\,m^2} = 0.59\,m/s$$

$$Q = V \times A \quad (7)$$

$$Q = 0.59\,m/s \times 0.0000282\,m^2 = 0.0000167\,m^3/s$$

Based on the approximate calculation of the radial air bearing flow rate, the required flow rate is 0.0000167 m³/s, which is equivalent to 1.002 LPM.

3.3 Testing

Testing was conducted to verify the design parameters of the radial air bearing system by comparing the results with the initial requirements. If there are deviations, the design and specifications can be adjusted until all parameters are met.

Fly height in an air bearing is the distance between the bearing surface and the related object. This distance needs to be considered based on the intended application. A fly height that is too low can lead to instability in the bearing. According to the New Way Air Bearing standard, the recommended fly height is 5 μm, with an ideal operating pressure range of 0.414 MPa to 0.61 MPa. To measure this distance, the shaft needs to be tested using a dial gauge with an accuracy of 0.001 mm on the upper surface. The fly height can be adjusted by the pressure exerted by the air bearing.

Table 6 presents data from an experiment related to the performance of an air bearing system. This table demonstrates the relationship between air pressure, flow rate, fly height, and shaft rotation in the EDM 10 system.

Table 6. Pressure variation data for EDM 10 Pad Materials

No.	Pressure (Bar)	Flowrate (LPM)		Fly height (μm)	Friction	Rotating shaft
1	4	MIN	2	2	Exist	No
2		MID	5	5	Exist	Yes (H)
3		MAX	9	9	Nothing	Yes (H)
4	5	MIN	2	2	Exist	No
5		MID	5	5	Exist	Yes (H)
6		MAX	12	12	Nothing	Yes
7	6	MIN	2	6	Exist	No
8		MID	5	12	Exist	Yes (H)
9		MAX	13	30	Nothing	Yes

*Remarks: H (Heavy) → The shaft turns with excessive resistance

The fly height remains at 2 μm under the MIN condition (4–5 bar), and as the flow rate increases to MID and MAX levels, the fly height increases to 5–12 μm. This study shows that the rig achieves stable lift at 4–5 bar pressure, with fly height increasing as airflow rises. These results align with another research on aerostatic bearings, which also found a link between supply pressure, flow rate, and bearing performance [12], [13]. This consistency supports the rig's reliability as a hands-on tool for learning how air bearings work. This behavior highlights the importance of optimizing air pressure to achieve ideal performance. At moderate pressure levels, the system reaches the recommended fly height of 5 μm, friction may still exist, and the shaft turns with excessive resistance. This behavior is attributed to the incomplete formation of a stable air film at main pressures and flow rates, which leads to boundary contact and friction. When operated at higher pressures, the fly height exceeds the standard, friction is eliminated, and the shaft rotates smoothly. The heavy rotational behavior is caused by insufficient lift force, resulting in partial contact between the shaft and bearing surface, which increases friction. Based on the data, the pressure-flowrate combination was unable to generate adequate lift, likely due to pressure drop across the pad. However, excessive pressure can potentially introduce rotational resistance or instability, emphasizing the need for careful calibration. The results indicate that increasing air pressure generally leads to a significant rise in both flow rate and fly height, as illustrated in Fig. 11.

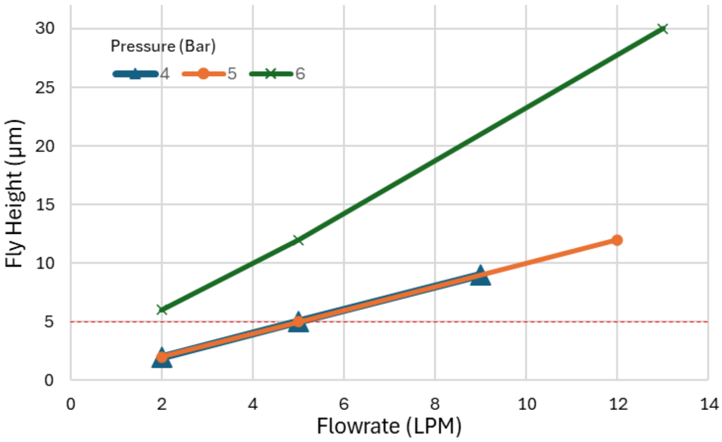

Fig. 11. Fly height vs. flow rate at varying pressure levels

These findings align with the New Way standard, which recommends a fly height of 5 μm at a pressure of 5 bar. Notably, the EDM 10 system demonstrates the capability to exceed this standard under higher pressure conditions, reaching up to 12 μm. This suggests enhanced lift performance, which could be advantageous for applications requiring greater clearance or reduced contact. From an educational perspective, this experiment provides a clear and practical demonstration of how design decisions and testing parameters influence system performance. It allows practitioners to observe the direct impact of pressure and flow rate on fly height and friction, reinforcing theoretical concepts with hands-on data.

4 Conclusions

The design of the radial air-bearing rig based on the New Way air-bearing standards has been successfully carried out in this study with a concave profile shape. The use of the VDI 2222 design methodology ensured a structured and thorough approach, covering planning, conceptualization, design, and finalization stages. The rig meets essential specifications, including pad material, flow rate, fly height, and air pressure input. This work lies in the integration of a concave bearing design, which is rarely explored in similar studies, and its potential use as an educational tool aid for engineering education. The system provides a practical platform for demonstrating the relationship between air pressure, lift, and friction, making it highly suitable for learning environments. Increasing air pressure improves flow rate and fly height while reducing friction. However, the resulting fly height often exceeds the standard 5 μm, reaching up to 30 μm, and may still cause friction and heavy shaft rotation. Friction occurs at low pressure due to an incomplete air film. At higher pressure, fly height increases and friction is reduced, but heavy rotation may still happen due to insufficient lift and pressure drop across the pad. Despite its success, the system still presents limitations, particularly in achieving consistent shaft rotation at the standard fly height due to residual friction. This indicates the need for further optimization, particularly in the formulation of the fly height and pressure requirement algorithms. Furthermore, integrating a control device for the pressure response of an air bearing system makes the system more adaptable for advanced research and industrial applications.

References

[1] H. Parshad, R. Kumar, and D. Dixit, "A Review on Air Bearing Working and Advantages," Jun. 2024.

[2] G. Chen, B. Ju, H. Fang, C. Yijie, N. Yu, and Y. Wan, "Air bearing: academic insights and trend analysis," *The International Journal of Advanced Manufacturing Technology*, vol. 106, Feb. 2020, doi: 10.1007/s00170-019-04663-5.

[3] C. Dong, C. Zhang, B. Wang, and G. Zhang, "Reducing the Dynamic Errors of Coordinate Measuring Machines," *Journal of Mechanical Design*, vol. 125, no. 4, pp. 831–839, Jan. 2004, doi: 10.1115/1.1623185.

[4] P. Zhang, "A study on accuracy of porous journal air bearing," *Precis Eng*, vol. 66, Jul. 2020, doi: 10.1016/j.precisioneng.2020.06.011.

[5] Truong Minh Duc, Vu Van Quang, Vu Toan Thang, and Le Cong Du, "A research of stabilization for high speed air bearing spindles," *Journal of Engineering and Science Research*, vol. 1, no. 2, pp. 228–233, 2017, doi: 10.26666/rmp.jesr.2017.2.34.

[6] Sakshi Potdar and Srinidhi Campli, "Air Bearings-Application Review," *International Journal of Science and Research (IJSR)*, vol. 10, no. 5, pp. 624–626, May 2021.

[7] R. Wong and U. N. Saraih, "Integrating Technology Skills with Interpersonal Competencies to Enhance Graduate Employability in Malaysian Technical Networks," *Finansha: Journal of Sharia Financial Management*, vol. 5, no. 2, pp. 204–219, Dec. 2024, doi: 10.15575/fjsfm.v5i2.41400.

[8] Darmawan Harsokoesoemo, *Pengantar Perancangan Teknik (Perancangan Produk)*, 2nd ed. Bandung: ITB, 2004.

[9] New Way Air Bearings, "Radial Air Bearing Application & Design Guide (Revision F)," USA, 2021. Accessed: Aug. 22, 2025. [Online]. Available: https://www.newwayairbearings.com/sites/default/files/new_way_application_and_design_guide_%20Rev_E_2006-01-18.pdf

[10] S. Fatmaryanti, "Development of Physics Teaching Media Using Speed Sensors as Speed Analysis in Realtime Based on Arduino to Remind Students' Problem Solving Abilities," *JIPF (Jurnal Ilmu Pendidikan Fisika)*, vol. 5, p. 151, Aug. 2020, doi: 10.26737/jipf.v5i3.1789.

[11] J. Natarajan and Dr. M. Aron Antony Charles, "Effective Teaching Through Media," *Quest Journals: Journal of Research in Humanities and Social Science*, vol. 9, no. 8, pp. 47–49, 2021.

[12] M. Ochiai, H. Sasaki, Y. Sunami, and H. Hashimoto, "Experimental and Theoretical Verification of Impact Response on Air Thrust Bearing with Topological Optimized Groove," *Tribology Online*, vol. 10, no. 2, pp. 115–120, 2015.

[13] J. Yin, J. Yu, P. Cao, D. Li, X. Shen, and M. Li, "Characteristics of Air Resistance in Aerostatic Bearings," *Applied Sciences*, vol. 11, no. 22, 2021, doi: 10.3390/app112210604.